Metallocenes of the alkaline earth metals and their carbene complexes

Herbert Schumann *, Jochen Gottfriedsen, Mario Glanz, Sebastian Dechert, Jörg Demtschuk

Institut für Anorganische und Analytische Chemie der Technischen Universität Berlin, Strasse des 17. Juni 135, 10623 Berlin, Germany

Abstract

Novel alkaline earth metallocenes with various cyclopentadienyl ligands and their carbene adducts with 1,3-di-*iso*-propyl-4,5-dimethylimidazol-2-ylidene (*i*Pr-carbene) are described. The syntheses of the magnesocenes $(C_5Me_4H)_2Mg$ (**1**), $(C_5Me_4tBu)_2Mg$ (**2**), and $(C_5H_3-1-(SiMe_3)-3-tBu)_2Mg$ (**3**) were carried out by reaction of the corresponding cyclopentadiene with dibutylmagnesium. The calcocenes $(C_5Me_4H)_2(NH_3)_2Ca$ (**6**), $(C_5Me_4H)_2(NH_3)(THF)Ca$ (**7**) and the barocene $(C_5Me_4tBu)_2(THF)_2Ba$ (**13**) were prepaired by reaction of calcium and barium, respectively, with the corresponding cyclopentadienes. Refluxing **7** in THF–toluene yielded the ammonia-free complex $(C_5Me_4H)_2(THF)Ca$ (**8**). Metathesis reaction of $(C_5Me_4iPr)Na$ with CaI_2 gave the calcocene $(C_5Me_4iPr)_2(THF)Ca$ (**9**). $(C_5Me_4tBu)_2(py)_2Ba$ (**14**) results from dissolving **13** in pyridine. 1,3-Di-*iso*-propyl-4,5-dimethylimidazol-2-ylidene reacted with **1**, **3**, **7**, **8**, **13**, and $(C_5Me_5)_2(THF)_2Sr$ in toluene or THF to give the air- and moisture-sensitive adducts $(C_5Me_4H)_2(iPr-carbene)Mg$ (**4**), $(C_5H_3-1-(SiMe_3)-3-tBu)_2(iPr-carbene)Mg$ (**5**), $(C_5Me_4H)_2(iPr-carbene)Ca$ (**10**), $(C_5Me_4iPr)_2(iPr-carbene)Ca$ (**11**), $(C_5Me_5)_2(iPr-carbene)Sr$ (**12**), and $(C_5Me_4tBu)_2(iPr-carbene)Ba$ (**15**). The novel compounds have been characterized by elemental analysis, mass spectrometry and NMR spectroscopy as well as the X-ray structures of the metallocenes (**1**, **2**, **6**, **9**, **13**) and the carbene adducts (**4**, **10**, **11**, **12**, **15**). © 2001 Elsevier Science B.V. All rights reserved.

Keywords: Metallocenes; Alkaline earth compounds; Carbene complexes; X-ray structures
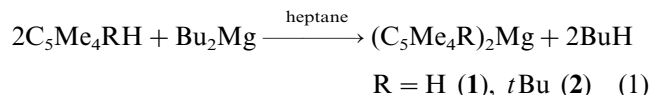
1. Introduction

Since the first isolation and X-ray structural characterization of free stable Wanzlick-carbenes [1] by Arduengo [2], a new area of very interesting transition metal complexes with these imidazolylidene type carbenes as ligands has developed [3]. Even stable adducts of elements like iodine [4], main group element derivatives like Me_3SiI, Ph_2SnCl_2 [5], electron-deficient moieties like BH_3 [6] as well as of the lanthanoids are known [7], demonstrating that this type of ligand is useful in the synthesis of carbene complexes with elements which are not capable of metal ligand π-back-bonding. Carbene complexes of $MgEt_2$ [8], alkaline earth metal amides [9] and $(C_5Me_5)_2M$ (M = Mg, Ca, Sr, Ba) [10] are also known employing tetramethyl-2-imidazolylidene as the

N-heterocyclic carbene. Herein we present the synthesis and characterization of a series of new metallocenes of the Group II elements and their corresponding carbene complexes, which have been used recently as catalysts for the activation of carbonyl groups [11].
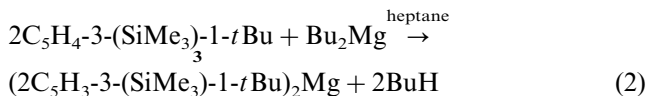
2. Results and discussion

2.1. Magnesium

Tetramethylcyclopentadiene, *tert*-butyl(tetramethyl)-cyclopentadiene, and 3-*tert*-butyl-1-(trimethylsilyl)-cyclopentadiene react with dibutylmagnesium in refluxing heptane yielding the base free magnesocenes **1**, **2**, and **3** (Eqs. (1) and (2)).

$$2C_5Me_4RH + Bu_2Mg \xrightarrow{\text{heptane}} (C_5Me_4R)_2Mg + 2BuH$$

$$R = H\ (\mathbf{1}),\ tBu\ (\mathbf{2}) \quad (1)$$

* Corresponding author. Tel.: +49-30-31423984; fax: +49-30-31422168.

E-mail address: schumann@chem.tu-berlin.de (H. Schumann).

$$2C_5H_4\text{-}3\text{-}(SiMe_3)\text{-}1\text{-}t\text{Bu} + Bu_2Mg \xrightarrow{\text{heptane}}$$

$$(2C_5H_3\text{-}3\text{-}(SiMe_3)\text{-}1\text{-}t\text{Bu})_2Mg + 2BuH \qquad (2)$$

Crystallization from heptane gave **1**–**3** as colorless crystalline compounds which are extremely sensitive to moisture and air. The complexes are soluble in polar solvents such as pyridine and THF as well as in non-polar and aromatic solvents such as hexane, toluene, and benzene. **1** and **2** sublime at 110°C and 160°C, respectively while **3** melts at 99°C. The ^1H- and ^{13}C-NMR signals are in the expected range. **3** reveals multiplets for the *tert*-butyl and the trimethylsilyl groups in the ^1H- and a double signal set in the ^{13}C-NMR spectra, demonstrating the hindered rotation
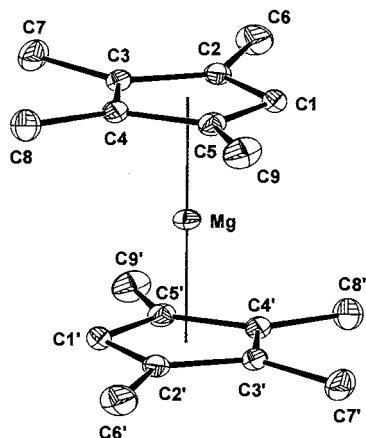

Fig. 1. ORTEP plot [12] of **1** with 30% probability thermal ellipsoids. Selected bond lengths [Å] and angles [°] (Cp and Cp′ were defined by the ring atoms C1–C5 and C1′–C5′): Mg–Cp 1.9702(4), Cp–Mg–Cp′ 180.0. Ring slippage [Å]: Cp 0.025. Symmetry transformations used to generate equivalent atoms: ′ $-x+1$, $-y+1$, $-z+1$.
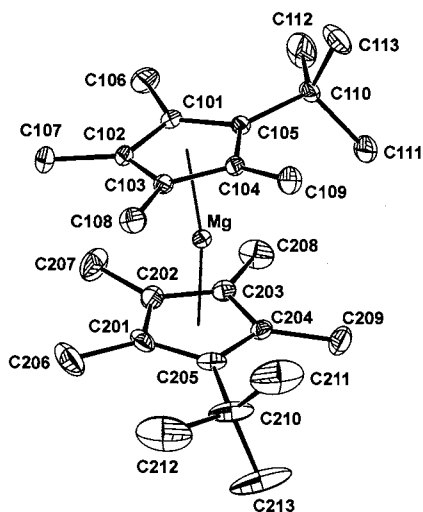

Fig. 2. ORTEP plot [12] of **2** with 30% probability thermal ellipsoids. Selected bond lengths [Å] and angles [°] (Cp1 and Cp2 were defined by the ring atoms C101–C105 and C201–C205): Mg–Cp1 1.9942(13), Mg–Cp2 1.9922(12), Cp1–Mg–Cp2 168.96(6). Ring slippage [Å]: Cp1 0.017, Cp2 0.029.

of the Cp rings at room temperature. The molecular ion is the peak of highest mass in all mass spectra with an intensity of 74–100%. Additionally a fragment formed by loss of one of the cyclopentadienyl ligands is found.

Crystals of **1** and **2** suitable for single-crystal X-ray diffraction analysis were obtained by crystallization from heptane. The structure of **1** is centrosymmetric with a Cp–Mg–Cp angle of 180° and a staggered conformation of the Cp rings (Fig. 1).

The distance of Mg to the planar η^5 bonded Cp rings is 1.97 Å. In contrast, the sterically demanding *tert*-butyl groups in **2** cause a bent geometry at the magnesium atom with an angle of 169° (Fig. 2). The Mg–Cp distance of 1.99 Å in **2** is in good agreement with those of **1** and of the known magnesocenes $(C_5H_5)_2Mg$ (1.99, 2.01 Å) [13], $(C_5Me_5)_2Mg$ (2.02 Å) [14] and $(C_5H_4t\text{Bu})_2Mg$ (2.00 Å) [15] with linear geometry at magnesium. The usage of bulky trimethylsilyl groups in $(C_5H_2\text{-}1,2,4\text{-}(SiMe_3)_3)_2Mg$ [16] results in slightly longer Mg–Cp bonds of 2.02–2.04 Å and an angle of 171° similar to that found in the structure of **2**.

These magnesocenes are good precursors for the synthesis of carbene complexes. Reactions of **1** and **3** with 1,3-di-*iso*-propyl-4,5-dimethylimidazol-2-ylidene (*i*Pr-carbene) give the corresponding carbene adducts **4** and **5** (Eqs. (3) and (4)).
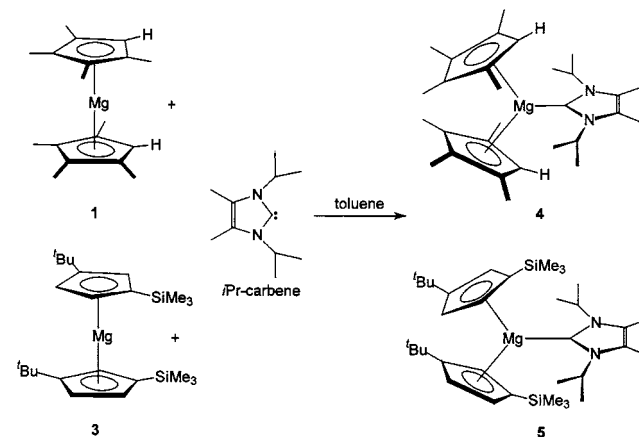
The colorless and crystalline **4** and **5** are also extremely air and moisture sensitive. They show good solubility in polar (THF, pyridine) and non-polar solvents (hexane, pentane, benzene, toluene). Both compounds melt without decomposition at 151°C (**4**) and 130°C (**5**), respectively. The mass spectra under electron ionization conditions show the carbene-free magnesocenes as the fragments with the highest mass. This phenomenon is also known from the carbene adducts of the lanthanoids [7]. Loss of the carbene ligand is prevented by use of chemical ionization as the ionization method: both molecular ions, **4** ($m/z = 445$) and **5** ($m/z = 590$), were found while the main fragmentation is the loss of a cyclopentadienyl ring. The ^1H-NMR
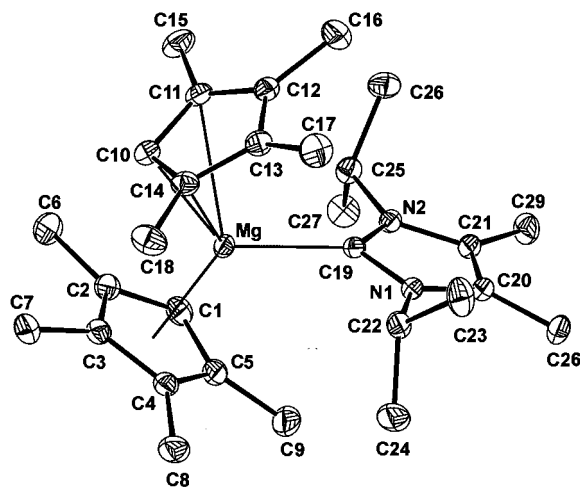
Fig. 3. ORTEP plot [12] of **4** with 30% probability thermal ellipsoids. Selected bond lengths [Å] and angles [°] (Cp1 and Cp2 were defined by the ring atoms C1–C5 and C10–C14, Cp2(η^3) was defined by the ring atoms C10, C11 and C14): Mg–Cp1 2.183(4), Mg–Cp2 2.222(4), Mg–C19 2.2260(13), N1–C19 1.3640(16), N2–C19 1.3611(16), Cp1–Mg–Cp2 141.59(3), N1–C19–N2 104.07(11). Ring slippage [Å]: Cp1 0.037, Cp2 0.807.
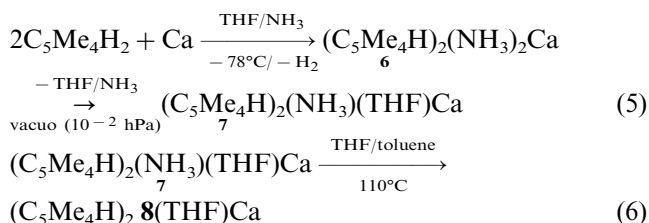
signals of the Cp ligand in **4** are found at a lower field than in **1** ($\Delta\delta$ 0.1–0.2 ppm). The corresponding ^{13}C signals also show a low field shift of 2–3 ppm, except for two ring signals which are shifted to higher field by 3–4 ppm. These data are in contrast to the results of **5** which give similar chemical shifts in the ^{1}H- and ^{13}C-NMR spectra as the homologous carbene-free magnesocene **3**, which shows two complete signal sets in the ^{13}C spectrum, whereas **5** gives only a doubled signal for the *t*Bu group at room temperature, demonstrating the influence of the carbene ligand on the dynamic rotation of the Cp ligands.

Crystals of **4** suitable for X-ray structure were grown from toluene at −25°C. In the solid state structure of **4** two different bonding modes for the Cp ligands are visible (Fig. 3). One of the planar rings is coordinated in η^5 fashion with a Mg–Cp distance of 2.18 Å. The second ring is slipped to an η^3 bond shown by a ring slippage value of 0.807 Å and an Mg–Cp distance of 2.22 Å. The difference between the shortest and longest Mg–C distance is 0.69 Å. As described for $(C_5Me_5)_2$-Mg(1,3,4,5-tetramethylimidazol-2-ylidene) [10], the slippage of one Cp ring is more due to an effect of metal size and steric bulk of the methylated Cp rings than to a C–C interaction between the Cp rings and the free p-orbital of the carbene carbon atom C19. The distance between magnesium and the C19 is 2.23 Å. The bond is slightly longer than in $(C_5Me_5)_2$Mg(1,3,4,5-tetramethylimidazol-2-ylidene) (2.19 Å) forced by the steric bulk of the *iso*-propyl groups. These groups are turned away from the magnesium center. In comparison to the structure parameters of **2**, the Mg–Cp distances in **4** are elongated by 0.21 to 0.25 Å while the

third ligand causes a bent structure with a Cp–Mg–Cp angle of 141.6°.

2.2. Calcium and strontium

Tetramethylcyclopentadiene reacts with calcium metal in a mixture of liquid ammonia and THF at −78°C, following the procedure for the synthesis of calcocene $(C_5H_5)_2$Ca(THF)$_2$ [17], yielding bis(tetramethylcyclopentadienyl)calcium. After 3 h stirring at −78°C, warming up to room temperature, further stirring for 12 h, and additional 12 h at room temperature, colorless crystals of $(C_5Me_4H)_2$Ca(NH$_3$)$_2$ (**6**) drop out from the clear solution. After decanting of the crystals and evaporation, colorless $(C_5Me_4H)_2$Ca(NH$_3$)(THF) (**7**) remains, which loses the coordinated ammonia after 12 h refluxing in a THF–toluene mixture forming colorless $(C_5Me_4H)_2$Ca(THF) (**8**) (Eqs. (5) and (6)).

$$2C_5Me_4H_2 + Ca \xrightarrow[-78°C/-H_2]{THF/NH_3} (C_5Me_4H)_2\underset{\mathbf{6}}{(NH_3)_2}Ca$$

$$\xrightarrow[\text{vacuo (10}^{-2}\text{ hPa)}]{-THF/NH_3} (C_5Me_4H)_2\underset{\mathbf{7}}{(NH_3)(THF)}Ca \qquad (5)$$

$$(C_5Me_4H)_2\underset{\mathbf{7}}{(NH_3)(THF)}Ca \xrightarrow[110°C]{THF/toluene}$$

$$(C_5Me_4H)_2 \, \mathbf{8}(THF)Ca \qquad (6)$$

The sterically more demanding $(C_5Me_4iPr)_2$(THF)Ca (**9**) was obtained by metathesis reaction of tetramethyl-*iso*-propylcyclopentadienyl sodium with calcium iodide in THF (Eq. (7)). After extraction with toluene **9** crystallized as air and moisture sensitive colorless crystals which melt at 175°C without decomposition.

$$2C_5Me_4iPrNa + CaI_2 \xrightarrow{THF} (C_5Me_4iPr)_2\underset{\mathbf{9}}{(THF)}Ca + 2NaI \qquad (7)$$
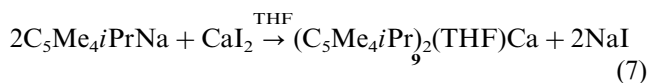
The mass spectra of **6**, **7**, **8** and **9** show the signal of highest mass for the molecular ion reduced by the mass of the solvent molecules. A loss of one Cp ligand is the main fragmentation in **9** shown by 100% intensity. The ^{1}H- and ^{13}C-NMR spectra show signals in the expected areas. The signals for the coordinated ammonia molecules were found at 1.49 ppm (pyridine-d_5) in **6** and at −0.11 ppm (benzene-d_6) in **7**.

Crystals of **6** grown from the ammonia saturated THF solution are suitable for X-ray structure determination. The calcium center is pseudo-tetrahedrally coordinated by two Cp and two NH$_3$ ligands with distances Ca–N of 2.48/2.50 and Ca–Cp 2.43/2.44 Å and angles N1–Ca–N2 of 87.6 and Cp1–Ca–Cp2 of 137.5° (Fig. 4). **9** shows a pseudo-trigonal planar geometry at calcium with Ca–Cp distances of 2.40 Å and a Cp–Ca–Cp′ angle of 143°, similar to that in **6** (Fig. 5). The structure parameters for **6** and **9** are similar to the known calcocenes with coordinated lewis bases like $(C_5H_3$-1,3-(SiMe$_3$)$_2$)$_2$(THF)Ca [18], $(C_5H_4tBu)_2$(THF)$_2$-

Ca [15], and $(C_5H_4Me)_2(DME)Ca$ [19], which show Ca–Cp and Ca–O distances in the range between 2.40 and 2.46 and 2.40 and 2.41 Å, respectively. The Cp–Ca–Cp angles of those calcocenes (133–135°) are slightly smaller than in **6** and **9**. Comparable structural data for the Ca–N bond are rare. The Ca–N distances in $[Ca\{(S)-\eta^5:\eta^1-C_5H_4(CHPhCH_2NMe_2)\}_2]$ are slightly larger (2.56 and 2.60 Å) than in **6**, probably forced by the methyl substitution at the nitrogen atoms [20]. $[Ca(N_3)_2(py)_2]$ [21] and $[Ca(N\text{-carbazolyl})_2(py)_4]$ [22] containing pyridine as coordinated Lewis base reveal Ca–N distances between 2.51 and 2.54 Å.
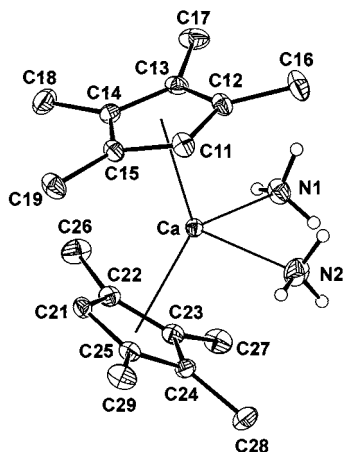

Fig. 4. ORTEP plot [12] of **6** with 30% probability thermal ellipsoids. Selected bond lengths [Å] and angles [°] (Cp1 and Cp2 were defined by the ring atoms C11–C15 and C21–C25): Ca–Cp1 2.4351(2), Ca–Cp2 2.4421(2), Ca–N1 2.4844(15), Ca–N2 2.5066(16), Cp1–Ca–Cp2 137.52(1), N1–Ca–N2 87.63(6). Ring slippage [Å]: Cp1 0.062, Cp2 0.151.
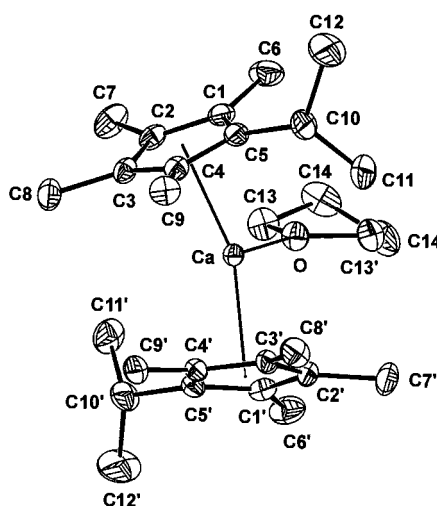

Fig. 5. ORTEP plot [12] of **9** with 30% probability thermal ellipsoids. Selected bond lengths [Å] and angles [°] (Cp and Cp′ were defined by the ring atoms C1–C5 and C1′–C5′): Ca–Cp 2.4010(5), Ca–O 2.408(2), Cp–Ca–Cp′ 142.97(2). Ring slippage [Å]: Cp 0.141. Symmetry transformations used to generate equivalent atoms: ′ $x - y$, $-y$, $-z + 2/3$.
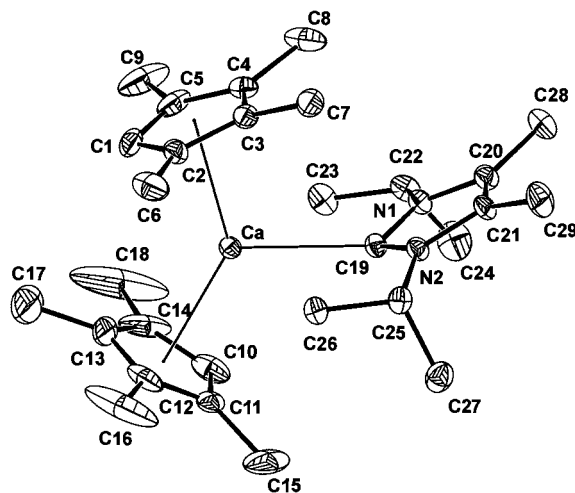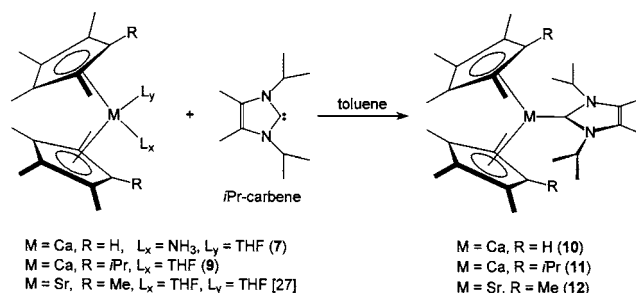

Fig. 6. ORTEP plot [12] of **10** with 30% probability thermal ellipsoids. Selected bond lengths [Å] and angles [°] (Cp1 and Cp2 were defined by the ring atoms C1–C5 and C10–C14, Cp1(η^3) was defined by the ring atoms C1, C2 and C5): Ca–Cp1 2.4501(18), Ca–Cp2 2.433(2), Ca–C19 2.593(4), Ca–C23 3.203(4), Ca–C26 3.088(4), N1–C19 1.362(4), N2–C19 1.360(4), Cp1–Ca–Cp2 135.49(8), N1–C19–N2 102.5(3). Ring slippage [Å]: Cp1 0.200, Cp2 0.081.

7 and **9** react with 1,3-di-*iso*-propyl-4,5-dimethylimidazol-2-ylidene in toluene at room temperature yielding the carbene adducts **10** and **11** (Eq. (8)), which crystallize from toluene at $-20°C$. Their mass spectra show the molecular ion reduced by the mass of the carbene ligand as the signals with the highest mass. The chemical shifts in the ^1H- and ^{13}C-NMR spectra for the *iso*-propyl group of **11** correspond to those for the free carbene signals. In contrast, those of **10** are shifted to higher field (0.3 ppm (^1H) and 3 ppm (^{13}C)). The signals of the carbene carbon bonded to the metal are shifted to higher field (190.53 ppm (**10**), 195.93 ppm (**11**)) compared to the free carbene (207.41 ppm).

M = Ca, R = H, L_x = NH$_3$, L_y = THF (**7**)
M = Ca, R = *i*Pr, L_x = THF (**9**)
M = Sr, R = Me, L_x = THF, L_y = THF [27]

M = Ca, R = H (**10**)
M = Ca, R = *i*Pr (**11**)
M = Sr, R = Me (**12**)

$$(8)$$

The molecular structures of **10** and **11** reveal a biscyclopentadienyl calcium unit coordinated by a carbene in a pseudo-trigonal planar fashion (Figs. 6 and 7). **11** crystallizes with two crystalline independent molecules in the unit cell; only one is shown in Fig. 7. The Ca–Cp distances of 2.43–2.45 Å for **10** and 2.43–2.44 Å for **11** are not influenced by the different kind of substitution at the Cp rings. Both Cp rings in **11** are η^5 bonded, whereas one of the Cp ligands (Cp1) in **10** shows a

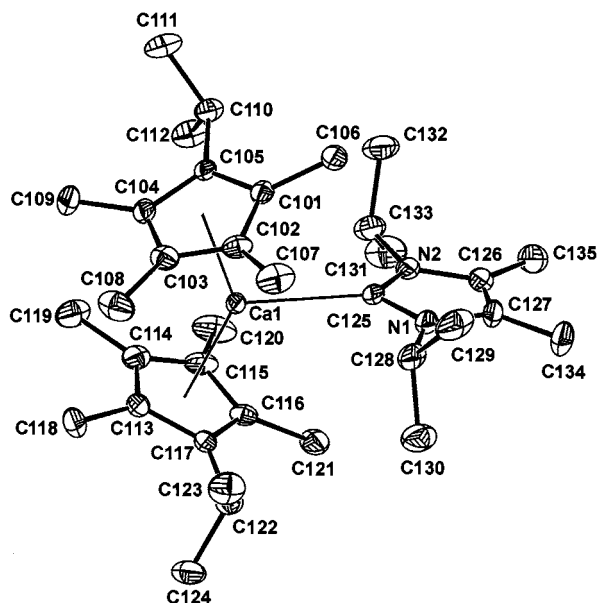tendency to η^3 bonding indicated by a high ring slippage value of 0.200 Å. This is compensated by an

Fig. 7. ORTEP plot [12] of **11** with 30% probability thermal ellipsoids. Only one of the two crystallographically independent molecules is shown. Selected bond lengths [Å] and angles [°] (Cp1 and Cp2 were defined by the ring atoms C101–C105 and C113–C117, Cp3 and Cp4 were defined by the atoms C201–C205 and C213–C125): Ca1–Cp1 2.4330(15) [Ca2–Cp3 2.4394(16)], Ca1–Cp2 2.4340(15) [Ca2–Cp3 2.4349(17)], Ca1–C125 2.674(3) [Ca2–C225 2.686(3)], N1–C125 1.355(4) [N3–C225 1.369(4)], N2–C125 1.378(4) [N4–C225 1.364(4)], Cp1–Ca1–Cp2 141.09(5) [Cp3–Ca2–Cp4 140.34(6)], N1–C125–N2 103.8(2) [N3–C225–N4 103.8(3)]. Ring slippage [Å]: Cp1 0.059 [Cp3 0.093], Cp2 0.023 [Cp4 0.035].
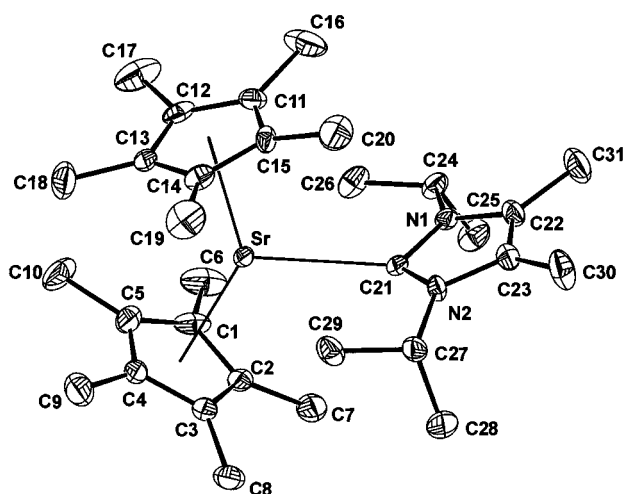

Fig. 8. ORTEP plot [12] of **12** with 30% probability thermal ellipsoids. Selected bond lengths [Å] and angles [°] (Cp1 and Cp2 were defined by the ring atoms C1–C5 and C11–C15): Sr–Cp1 2.576(3), Sr–Cp2 2.593(2), Sr–C21 2.768(4), Sr–C26 3.235(6), Sr–C29 3.240(6), N1–C21 1.364(6), N2–C21 1.350(6), Cp1–Sr–Cp2 139.47(8), N1–C19–N2 102.7(4). Ring slippage [Å]: Cp1 0.065, Cp2 0.099.

interaction between one CH_3 group of each *iso*-propyl group with the calcium center leading to Ca–CH_3 distances of 3.09 and 3.20 Å and a high field shift in the NMR spectra. The steric bulk of the Cp ligands in **11** does not allow such an interaction. The carbene *iso*-propyl groups are bent away from calcium and the Cp–Ca–Cp angles are 140–141° compared to 135.5° in **10**. Also the carbene carbon distances in **10** are slightly shorter (2.59 Å) than in **11** (2.67–2.69 Å). This is in good agreement with the ^{13}C-NMR results, with the stronger bond in **10** leading to a greater high field shift. The different bond strength is caused by the steric bulk of the *iso*-propyl groups of the carbene ligand. In $(C_5Me_5)_2(1,3,4,5$-tetramethylimidazol-2-ylidene)Ca [10] an even smaller Ca–C(carbene) distance of 2.56 Å was found with a sterically less hindered carbene.

The colorless, air- and moisture-sensitive bis(pentamethylcyclopentadienyl)strontium carbene adduct **12** is soluble in polar and aromatic solvents, but not in alkanes. The mass spectrum shows $(C_5Me_5)_2Sr$ as highest detectable mass in the electron ionization mass spectra. The molecular ion is only visible under chemical ionization conditions. In the latter case, the peak of highest abundance is due to loss of one C_5Me_5 ligand. As in **10** the signals of the *iso*-propyl groups are shifted to higher field compared to the free carbene in ^{1}H- and ^{13}C-NMR spectra. No signal attributable to the carbene carbon was found.

The X-ray structure of **12** reveals the same metal carbon interaction as for the CH_3 units of the *iso*-propyl groups in the Ca complex (**10**) indicated by the short Sr–C distances in **12** of 3.23 and 3.24 Å (Fig. 8). The Sr–Cp bond (2.58 and 2.60 Å), and the Cp–Sr–Cp angle of 139.5° are in the typical range for biscyclopentadienyl strontium Lewis base adducts, e.g. $(C_5H_3$-1,3-$(SiMe_3)_2)_2$(THF)Sr [18a] (2.61 Å, 133°), $(C_5H_4tBu)_2$-(THF)$_2$Sr [15] (2.55 Å, 134°), and $(C_5H_3$-1,2,4-$iPr_3)_2$(THF)Sr [23] (2.57 Å, 139°). As expected, the Sr–C(carbene) distance of 2.77 Å in the pseudo-trigonal planar coordinated complex **12** is shorter than in the pseudo-tetrahedral $(C_5Me_5)_2(1,3,4,5$-tetramethylimidazol-2-ylidene)$_2$Sr (2.85–2.87 Å) [10].

2.3. Barium

The THF adduct $(C_5Me_4tBu)_2$(THF)$_2$Ba (**13**) was synthesized from barium metal in an ammonia saturated THF solution and crystallized from toluene (Eq. (9)) as colorless air- and moisture-sensitive crystals melting at 180°C. As highest mass in the EI mass spectrum $(C_5Me_4tBu)_2$Ba is found forming from the molecular ion under loss of THF. The stronger base pyridine replaces both THF ligands dissolving **13** in pyridine. $(C_5Me_4tBu)_2(NC_5H_5)_2$Ba (**14**) was obtained as yellow crystals (Eq. (10)).

Fig. 9. ORTEP plot [12] of **14** with 30% probability thermal ellipsoids. Selected bond lengths [Å] and angles [°] (Cp1 and Cp2 were defined by the ring atoms C101–C105 and C201–C205): Ba–Cp1 2.7886(16), Ba–Cp2 2.7959(19), Ba–N1 2.932(3), Ba–N2 2.927(3), Cp1–Ba–Cp2 140.26(5), N1–Ba–N2 79.28(10). Ring slippage [Å]: Cp1 0.089, Cp2 0.065.
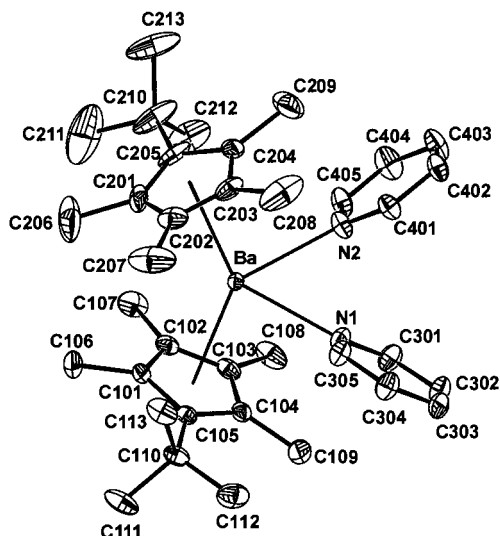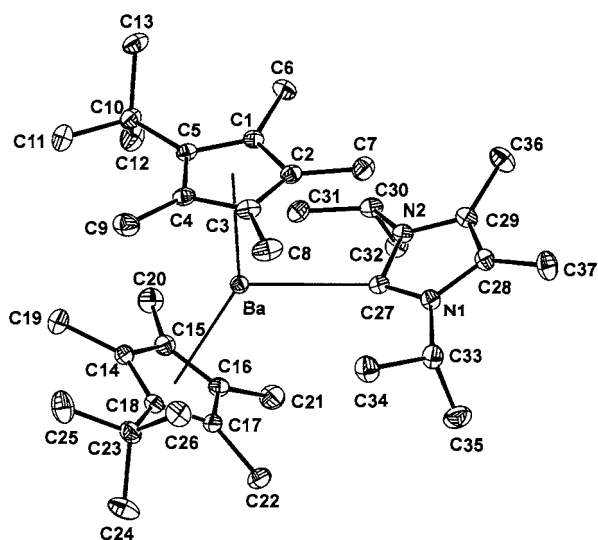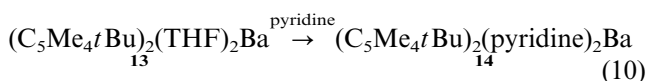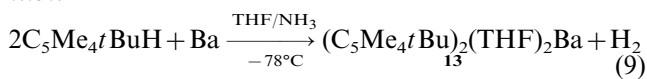

Fig. 10. ORTEP plot [12] of **15** with 30% probability thermal ellipsoids. Selected bond lengths [Å] and angles [°] (Cp1 and Cp2 were defined by the ring atoms C1–C5 and C14–C18): Ba–Cp1 2.7906(13), Ba–Cp2 2.7573(13), Ba–C27 3.002(3), Ba–C31 3.316(3), Ba–C34 3.515(4), N1–C27 1.367(4), N2–C27 1.369(4), Cp1–Ba–Cp2 148.04(4), N1–C27–N2 102.4(2). Ring slippage [Å]: Cp1 0.067, Cp2 0.030.

$$2C_5Me_4tBuH + Ba \xrightarrow[-78°C]{THF/NH_3} \underset{\mathbf{13}}{(C_5Me_4tBu)_2(THF)_2Ba} + H_2 \quad (9)$$

$$\underset{\mathbf{13}}{(C_5Me_4tBu)_2(THF)_2Ba} \xrightarrow{pyridine} \underset{\mathbf{14}}{(C_5Me_4tBu)_2(pyridine)_2Ba} \quad (10)$$

13 and **14** are soluble in the polar solvents THF and pyridine, less soluble in aromatic solvents like toluene or benzene, and not at all soluble in aliphatic hydrocar-

bons. In the EI mass spectrum of both compounds only $(C_5Me_4tBu)_2Ba$ without any donor molecules can be detected.

The X-ray structure of **14** (Fig. 9) shows the same pseudo-tetrahedral geometry as the known $(C_5iPr_3H_2)_2$-$(THF)_2Ba$ [24]. The Ba–Cp distances (2.79–2.80 Å) are approximately the same, while the Cp–Ba–Cp angle (140°) is larger by 8°, probably because the planar pyridine is sterically less demanding than the bent THF ring. The Ba–N distance (2.93 Å) is slighty longer than in $[\{(C_5Me_5)_2Ba\}_2(\mu-NC_6H_4N)]$ (2.87 Å) [25].

In contrast to the synthesis of the magnesium, calcium and strontium carbene complexes, **13** does not react with 1,3-di-*iso*-propyl-4,5-dimethylimidazol-2-yli-dene in toluene at room temperature. But refluxing the educts yields the carbene adduct **15** (Eq. (11)) in the form of colorless highly air- and moisture-sensitive crystals, which is in contrast to the complexes **13** and **14** very soluble in aromatic solvents. The ^{1}H- and ^{13}C-NMR spectra show the methyl signals of the carbene *iso*-propyl groups high field shifted by 0.3 ppm (^{1}H) and 1.2 ppm (^{13}C) compared to the free carbene ligand, like in the homologous Ca and Sr complexes **10** and **12**.

$$(11)$$
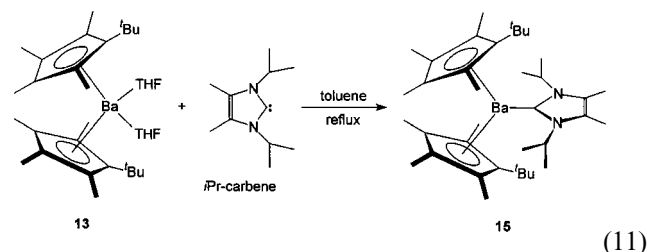
The X-ray structure determination of **15** reveals monomeric molecules with pseudo-trigonal planar geometry leading to an 8° increase of the Cp–Ba–Cp angle (148°) compared to **14** (Fig. 10). The Ba–Cp distances (2.79 and 2.76 Å) are equivalent to those in **14**. Like in the structures of **10** and **12**, two CH_3 groups in **15** are orientated to the Ba center with Ba–C distances of 3.32 and 3.52 Å, respectively. The structure of **15** exhibits a slightly longer Ba–C(carbene) bond distance (3.00 Å) than in $(C_5Me_5)_2(C_7H_{12}N_2)Ba$ (2.95 Å) [10].

3. Conclusion

A series of new alkaline earth metallocenes forms carbene adducts with 1,3-di-*iso*-propyl-4,5-dimethylimi-dazoly-2-ylidene. Comparative X-ray and NMR studies confirm the dependence of the metal carbene bond strength on the alkaline earth metal size also found by Arduengo et al. [10]. Additionally the employment of different ligands especially within the calcium complexes **10** and **11** reveals a relation to the steric demand

of the Cp ligand shown by the metal–carbene distances under consideration of the effective ionic radii [26] and the ^{13}C-NMR shift of the carbene carbon (Table 1). Bulky Cp ligands cause longer metal to carbene carbon bonds. The Lewis-acidic metals compensate their electron deficiency by interaction with the *iso*-propyl-methyl groups of the carbene ligands if the coordination sphere allows an approach of the *iso*-propyl groups towards the metal center. The metal cyclopentadienyl distance remains basically unchanged whether a carbene, THF or pyridine molecule is bond as the Lewis base. An exceptional behavior is shown by the magnesocene carbene adducts in comparison with the base free magnesocenes: the Mg–C bond is elongated by 0.2 Å after carbene coordination.

4. Experimental

4.1. General

All operations were performed under an inert atmosphere of dry argon using Schlenk techniques. Solvents were dried and distilled according to standard procedures. The ^{1}H- and ^{13}C-NMR spectra were recorded with the Bruker ARX 200 (^{1}H, 200 MHz; ^{13}C, 50.32 MHz), and ARX 400 (^{1}H, 400 MHz; ^{13}C, 100.64 MHz) instruments, calibrated against the residual protons of the carefully dried deuterated solvents. Elemental analysis were carried out at a Perkin–Elmer Series II CHNS/O Analyzer 2400. Mass spectra under electron ionization conditions (EI 70 eV) were recorded with a Varian MAT 311 A mass spectrometer. The mass spectra of **10**, **13**, and **15** were recorded with a modified VG-ZAB-HF/AMD-604 four-sector mass spectrometer [27] under chemical ionization conditions with methane as a reagent gas (CI 100 eV energy, repeller ca. 0 V, p(methane) = 10^{-4} hPa). Tetramethyl(*tert*-butyl)cyclopentadiene [28], 3-*tert*-butyl(1-trimethylsilyl)cyclopentadiene [29], tetramethyl-(*iso*-propyl)cyclopentadienyl-sodium [30], bis(pentamethylcyclopentadienyl)bis-(tetrahydrofuran)strontium [31], and 1,3-di-*iso*-propyl-4,5-dimethylimidazol-2-ylidene [32] were synthesized according to the literature.

4.2. Synthesis

4.2.1. (C$_5$Me$_4$H)$_2$Mg (1)

5 ml of a solution of Bu$_2$Mg in heptane ($c = 1$ mol l^{-1}) were added to 1.24 g (10.1 mmol) of C$_5$Me$_4$H$_2$ and refluxed for 12 h. A colorless solid was obtained by crystallization at -20°C from heptane. The clear solution was decanted and the colorless crystals were dried in vacuo (10^{-2} hPa). Yield: 2.45 g (91%). Subl.: 110°C (10^{-2} hPa). Anal. Calc. for C$_{18}$H$_{26}$Mg: C, 81.06; H, 9.83. Found: C, 80.70; H, 9.53%. ^{1}H-NMR (benzene-d_6, 200 MHz): δ 5.46 (s, 2H, Cp*H*), 1.98 (s, 12H, CpC*H*$_3$), 1.89 (s, 12H, CpC*H*$_3$). ^{13}C{^{1}H} (benzene-d_6, 50.32 MHz): δ 112.35 (*C*$_5$CH$_3$), 112.18 (*C*$_5$CH$_3$), 101.95 (*C*$_5$H), 11.52 (*C*H$_3$), 9.54 (*C*H$_3$). MS (EI, ^{24}Mg, 91°C): m/z 266 (87%) [M]$^+$, 145 (25%) [C$_9$H$_{13}$Mg]$^+$, 122 (100%) [C$_9$H$_{14}$]$^+$.

4.2.2. (C$_5$Me$_4$tBu)$_2$Mg (2)

Analogously to **1** 1.72 g (9.6 mmol) C$_5$Me$_4$*t*BuH was reacted with 4.8 ml Bu$_2$Mg in heptane (1.0 mol l^{-1}). Crystallization at -78°C gave **2** as colorless crystals. Yield: 1.56 g (43%). Subl.: 160°C (10^{-2} hPa). Anal. Calc. for C$_{26}$H$_{42}$Mg: C, 82.41; H, 11.17. Found: C, 81.83; H, 11.05%. ^{1}H-NMR (benzene-d_6, 200 MHz): δ 2.14 (s, 12H, Cp(C*H*$_3$)$_2$), 1.96 (s, 12H, Cp(C*H*$_3$)$_2$), 1.39 (s, 18H, C(C*H*$_3$)$_3$). ^{13}C{^{1}H} (benzene-d_6, 50.32 MHz): δ 122.62 (*C*$_5$CCH$_3$), 112.98 (*C*$_5$CH$_3$), 110.15 (*C*$_5$CH$_3$), 35.07 (*C*CH$_3$), 33.28 (C*C*H$_3$), 14.19 (*C*$_5$CH$_3$), 10.84 (*C*$_5$CH$_3$). MS (EI, ^{24}Mg, 122°C): m/z 378 (100%) [M]$^+$, 363 (92%) [M$-$CH$_3$]$^+$, 321 (10%) [M$-$C$_4$H$_9$]$^+$, 307 (31%) [M$-$C$_4$H$_9$$-CH_3$]$^+$, 201 (24%) [C$_{13}H_{21}$Mg]$^+$.

4.2.3. (C$_5$H$_3$-1-(SiMe$_3$)-3-tBu)Mg (3)

Analogously to **1** 1.67 g (8.6 mmol) 3-*tert*-butyl-1-trimethylsilylcyclopentadiene was reacted with 4.3 ml Bu$_2$Mg in heptane (1.0 mol l^{-1}). Crystallization at -78°C gave **3** as colorless crystals. Yield: 3.15 g (89%). M.p.: 99°C. Anal. Calc. for C$_{24}$H$_{42}$MgSi$_2$: C, 70.12; H, 10.30. Found: C, 68.46; H, 9.67%. ^{1}H-NMR (benzene-d_6, 400 MHz): δ 6.29 (m, 2H, 2-Cp*H*), 6.20 (m, 4H, 4,5-Cp*H*), 1.27 (m, 18H, C(C*H*$_3$)$_3$), 0.31 (m, 18H, SiC*H*$_3$)$_3$). ^{13}C{^{1}H} (benzene-d_6, 100.64 MHz): δ 138.80 (*C*$_5$CCH$_3$), 138.66 (*C*$_5$CCH$_3$), 115.58 (*C*$_5$SiCH$_3$), 115.39 (*C*$_5$SiCH$_3$), 114.74 (2-*C*$_5$H), 114.65 (2-*C*$_5$H), 110.09 (4-

Table 1
Selected bond lengths and chemical shifts of the Group II metallocene carbene adducts (n.f. not found)

Compound	M–C(carbene) (Å)	M–C(carbene) (Å) eff. i.r.	^{13}C-NMR shift C(carbene) (ppm)
4	2.23		n.f.
10	2.59	1.53	190.53
11	2.66/2.67	1.60	195.93
12	2.77	1.56	n.f.
15	3.00	1.62	200.42

C_5H), 110.06 (4-C_5H), 108.55 (5-C_5H), 108.53 (5-C_5H), 32.350 (CCH_3), 32.345 (CCH_3), 0.488 (SiCH_3), 0.481 (SiCH_3). MS (EI, ^{24}Mg, 60°C): m/z 410 (74%) [M]$^+$, 395 (100%) [M $-$ CH$_3$]$^+$, 217 (10%) [M $-$ C$_{12}$H$_{21}$Si]$^+$, 201 (14%) [C$_{11}$H$_{18}$SiMg]$^+$.

4.2.4. ($C_5Me_4H)_2(iPr$-carbene)Mg (4)

iPr-carbene (0.64 g (3.6 mmol)) was added in portions to 0.96 g (3.6 mmol) of 1 dissolved in 25 ml THF. The mixture was stirred for 12 h at room temperature followed by removal of the solvent in vacuo (10^{-2} hPa). The remaining solid was dissolved in 3 ml of toluene and the following crystallization gave 4 as colorless crystals. Yield: 1.27 g (79%). M.p.: 151°C. Anal. Calc. for C$_{29}$H$_{46}$MgN$_2$: C, 77.92; H, 10.37; N, 6.27. Found: C, 76.91; H, 9.87; N, 6.57%. ^{1}H-NMR (benzene-d_6, 200 MHz): δ 5.55 (s, 2H, CpH), 3.92 (sept., $^3J(^1$H, ^{1}H) = 6.8 Hz, 2H, NCH(CH$_3$)$_2$), 2.19 (s, 12H, Cp(CH_3)$_2$), 2.10 (s, 12H, Cp(CH_3)$_2$), 1.58 (s, 6H, NC(CH_3)), 1.32 (d, $^3J(^1$H, ^{1}H) = 6.8 Hz, 12H, CH(CH_3)$_2$). ^{13}C{^{1}H} (benzene-d_6, 50.32 MHz): δ 123.34 (CCH$_3$), 114.73 (C_5CH$_3$), 111.66 (C_5CH$_3$), 97.47 (C_5), 51.72 (NCH), 23.66 (NCHCH$_3$), 13.46 (C_5CH$_3$), 11.98 (C_5CH$_3$), 9.52 (CCH_3). MS (CI, ^{24}Mg, 85°C): m/z 445 [M]$^+$, 325 [C$_{20}$H$_{33}$N$_2$Mg]$^+$, 204 [C$_{11}$H$_{20}$N$_2$Mg]$^+$.

4.2.5. (C_5H_3-1-(SiMe$_3$)-3-tBu)$_2$(iPr-carbene)Mg (5)

iPr-carbene (0.49 g (1.2 mmol)) was added in portions to 0.22 g (126 mmol) of 3 dissolved in 20 ml toluene. After stirring the mixture for 12 h at room temperature the mixture was concentrated in vacuo (10^{-2} hPa). Crystallization at -20°C gave 5 as a white solid. Yield: 0.37 g (75%). M.p.: 130°C. Anal. Calc. for C$_{35}$H$_{62}$MgN$_2$Si$_2$: C, 71.09; H, 10.57; N, 4.74. Found: C, 69.08; H, 10.14; N, 5.18%. ^{1}H-NMR (benzene-d_6, 200 MHz): δ 6.30 (m, 2H, 2-CpH), 6.22 (m, 4H, 4,5-Cp(H)$_2$), 3.98 (sept., $^3J(^1$H, ^{1}H) = 6.3 Hz, 2H, NCH(CH$_3$)$_2$), 1.70 (s, 6H, NC(CH_3)), 1.46 (d, $^3J(^1$H, ^{1}H) = 6.3 Hz, 12H, CH(CH_3)$_2$), 1.29 (s, 18H, C(CH_3)$_3$), 0.31 (s, 18H, Si(CH_3)$_3$). ^{13}C{^{1}H} (benzene-d_6, 50.32 MHz): δ 138.97 (C_5CCH$_3$), 138.83 (C_5CCH$_3$), 121.96 (NCCH$_3$), 115.46 (C_5SiCH$_3$), 114.47 (2-C_5H), 110.48 (4-C_5H), 108.49 (5-C_5H), 48.89 (NCH), 32.38 (CCH$_3$), 24.43 (NCHCH$_3$), 8.93 (CCH$_3$), 0.62 (SiCH$_3$), n.f. (NCN). MS (CI, ^{24}Mg): m/z 590 [M]$^+$.

4.2.6. ($C_5Me_4H)_2(NH_3)_2$Ca (6) and ($C_5Me_4H)_2(NH_3)(THF)$Ca (7)

Calcium pieces (1.10 g (27.0 mmol)) and C$_5$Me$_4$H$_2$ (6.6 g (54 mmol)) were stirred in 15 ml of THF. Ammonia was condensed at -78°C into this mixture for 20 min Ca dissolved and a golden solid was formed. After stirring for 3 h at -78°C the mixture was warmed up to 25°C and stirred for another 12 h. After further 12 h without stirring at room temperature, 0.5 g (6%) colorless crystals of 6 precipitated. M.p.: 214°C.

Anal. Calc. for C$_{18}$H$_{32}$CaN$_2$: C, 68.30; H, 10.19; N, 8.85. Found: C, 67.78; H, 10.56; N, 5.67%. ^{1}H-NMR (pyridine-d_5, 200 MHz): δ 5.75 (s, 2H, CpH), 3.66 (m, 1H, THF), 2.23 (s, 12H, Cp-1,4-(CH_3)$_2$), 1.98 (s, 12H, Cp-2,3-(CH_3)$_2$), 1.63 (m, 1H, THF), 1.49 (s$_{br}$, 6H, NH$_3$). ^{13}C{^{1}H} (pyridine-d_5, 50.32 MHz): δ 112.44 (C_5CH$_3$), 111.14 (C_5CH$_3$), 106.20 (C_5), 67.44 (THF), 25.39 (THF), 13.32 (CH$_3$), 11.17 (CH$_3$). MS (EI, ^{40}Ca, 292°C): m/z 281 (1%) [M $-$ 2NH$_3$$-$H]$^+$, 207 (2%) [C$_{13}H_{11}$Ca]$^+$, 122 (6%) [C$_9H_{14}$]$^+$.

The remaining clear solution was decanted and the solvents were removed in vacuo (10^{-2} hPa) followed by washing the remaining solid with pentane (3 $\times$) yielding 7 as a white powder. Yield: 8.4 g (84%). M.p.: 200°C. Anal. Calc. for C$_{22}$H$_{37}$CaNO: C, 71.11; H, 10.04; N, 3.77. Found: C, 70.00; H, 9.30; N, 3.41%. ^{1}H-NMR (benzene-d_6, 200 MHz): δ 5.57 (s, 2H, CpH), 3.22 (m, 4H, THF), 2.16 (s, 12H, Cp-1,4-(CH_3)$_2$), 1.98 (s, 12H, Cp-2,3-(CH_3)$_2$), 1.27 (m, 4H, THF), -0.11 (s$_{br}$, 3H, NH$_3$). ^{13}C{^{1}H} (benzene-d_6, 50.32 MHz): δ 112.62 (C_5CH$_3$), 111.67 (C_5CH$_3$), 106.35 (C_5), 68.48 (THF), 25.37 (THF), 13.47 (CH$_3$), 11.59 (CH$_3$). ^{1}H-NMR (pyridine-d_5, 200 MHz): δ 5.76 (s, 2H, CpH), 3.66 (m, 4H, THF), 2.22 (s, 12H, Cp-1,4-(CH_3)$_2$), 1.90 (s, 12H, Cp-2,3-(CH_3)$_2$), 1.76 (s$_{br}$, 3H, NH$_3$), 1.63 (m, 4H, THF). ^{13}C{^{1}H}(pyridine-d_5, 50.32 MHz): δ 112.44 (C_5CH$_3$), 111.14 (C_5CH$_3$), 106.20 (C_5), 67.44 (THF), 25.39 (THF), 13.32 (CH$_3$), 11.17 (CH$_3$). MS (EI, ^{40}Ca, 300°C): m/z 282 (4%) [M $-$ THF$-$NH$_3$]$^+$, 281 (7%) [M $-$ THF$-$NH$_3$$-$H]$^+$, 207 (45%) [C$_{13}H_{11}$Ca]$^+$, 122 (27%) [C$_9H_{14}$]$^+$.

4.2.7. ($C_5Me_4H)_2(THF)$Ca (8)

1.10 g (3.0 mmol) of 7 were dissolved in a mixture of 15 ml toluene and 15 ml THF followed by refluxing for 12 h. The solvents were removed in vacuo (10^{-2} hPa) followed by addition of 5 ml toluene and 5 ml hexane. At -20°C 8 was isolated as colorless crystals. Yield: 1.00 g (100%). M.p.: 101°C. Anal. Calc. for C$_{22}$H$_{34}$CaO: C, 74.52; H, 9.66. Found: C, 73.40; H, 10.18%. ^{1}H-NMR (benzene-d_6, 200 MHz): δ 5.62 (s, 2H, CpH), 3.29 (m, 4H, THF), 2.20 (s, 12H, Cp(CH_3)$_2$), 2.08 (s, 12H, Cp(CH_3)$_2$), 1.29 (m, 4H, THF). ^{13}C{^{1}H} (benzene-d_6, 50.32 MHz): δ 113.90 (C_5CH$_3$), 112.71 (C_5CH$_3$), 107.17 (C_5), 68.95 (THF), 25.16 (THF), 13.26 (CH$_3$), 11.48 (CH$_3$). MS (EI, ^{40}Ca, 277°C): m/z 282 (10%) [M $-$ THF]$^+$, 281 (9%) [M $-$ THF$-$H]$^+$, 207 (34%) [C$_{13}$H$_{11}$Ca]$^+$, 122 (28%) [C$_9$H$_{14}$]$^+$.

4.2.8. ($C_5Me_4iPr)_2(THF)$Ca (9)

To a solution of 1.03 g (5.5 mmol) (C$_5$Me$_4$$i$Pr)Na in 30 ml THF, 0.81 g (2.8 mmol) of CaI$_2$ was added in portions. After stirring the mixture for 12 h at 25°C, the THF was removed in vacuo (10^{-2} hPa) followed by continuous extraction with 50 ml of toluene. The clear

solution was concentrated to 10 ml. Crystallization at $-20\,^{\circ}$C yielded **9** as colorless crystals. Yield: 0.57 g (47%). M.p.: 175°C. Anal. Calc. for $C_{28}H_{46}CaO$: C, 76.65; H, 10.57. Found: C, 75.86; H, 11.03%. ^{1}H-NMR (benzene-d_6, 200 MHz): δ 3.30 (m, 4H, THF), 3.05 (sept., $^3J(^1H, {}^1H) = 7.1$ Hz, 2H, CH(CH$_3$)$_2$), 2.14 (s, 12H, Cp(CH_3)$_2$), 2.06 (s, 12H, Cp(CH_3)$_2$), 1.28 (d, $^3J(^1H, {}^1H) = 7.1$ Hz, 12H, CH(CH_3)$_2$), 1.27 (m, 4H, THF). ^{13}C$\{^1$H$\}$ (benzene-d_6, 50.32 MHz): δ 122.15 (C_5CHCH$_3$), 112.53 (C_5CH$_3$), 112.28 (C_5CH$_3$), 68.86 (THF), 27.13 (CHCH$_3$), 25.34 (THF), 23.77 (CHCH$_3$), 12.15 (C$_5$$CH_3$), 11.23 (C$_5$$CH_3$). MS (EI, ^{40}Ca, 125°C): m/z 366 (70%) [M $-$ THF]$^+$, 351 (6%) [M $-$ THF $-$ CH$_3$]$^+$, 203 (100%) [C$_{12}$H$_{19}$Ca]$^+$, 163 (48%) [C$_{12}$H$_{19}$]$^+$.

4.2.9. (C$_5$Me$_4$H)$_2$(iPr-carbene)Ca (10)

To 0.78 g (2.1 mmol) of **7** dissolved in 30 ml toluene, 0.37 g (2.1 mmol) of *i*Pr-carbene was added in portions. After stirring for 12 h at room temperature the mixture was concentrated in vacuo (10^{-2} hPa) to 10 ml. Colorless crystals of **10** were isolated at $-20\,^{\circ}$C. Yield: 1.05 g (88%). M.p.: 145°C. Anal. Calc. for $C_{29}H_{46}CaN_2$: C, 75.27; H, 10.02; N, 6.05. Found: C, 74.11; H, 10.42; N, 6.04%. ^{1}H-NMR (benzene-d_6, 400 MHz): δ 5.83 (s, 2H, CpH), 3.68 (sept., $^3J(^1H, {}^1H) = 6.5$ Hz, 2H, NCH(CH$_3$)$_2$), 2.25 (s, 12H, Cp(CH_3)$_2$), 2.10 (s, 12H, Cp(CH_3)$_2$), 1.54 (s, 6H, NC(CH_3)), 1.14 (d, $^3J(^1H, {}^1H) = 6.5$ Hz, 12H, NCH(CH_3)$_2$). ^{13}C$\{^1$H$\}$ (benzene-d_6, 100.64 MHz): δ 190.53 (NCN), 123.97 (NCCH$_3$), 113.53 (C_5CH$_3$), 112.39 (C_5CH$_3$), 107.00 (C_5H), 50.19 (NCH), 21.60 (NCHCH$_3$), 13.21 (C$_5$$CH_3$), 11.55 (C$_5$$CH_3$), 8.64 (C$CH_3$). MS (EI, ^{40}Ca, 128°C): m/z 282 (17%) [M $-$ C$_{11}$H$_{20}$N$_2$]$^+$, 180 (29%) [C$_{11}$H$_{20}$N$_2$]$^+$, 161 (46%) [C$_9$H$_{13}$Ca]$^+$, 122 (66%) [C$_{19}$H$_{14}$]$^+$.

4.2.10. (C$_5$Me$_4$iPr)$_2$(iPr-carbene)Ca (11)

Analogously to **10**, 0.91 g (2.1 mmol) of **9** was reacted with 0.37 g (2.1 mmol) of *i*Pr-carbene in 30 ml of toluene. The solvent was concentrated in vacuo (10^{-2} hPa) to 10 ml. Crystallization at $-20\,^{\circ}$C yields **11** as colorless crystals. Yield: 1.05 g (91%). M.p.: 138°C. Anal. Calc. for $C_{35}H_{58}CaN_2$: C, 76.68; H, 10.69; N, 5.12. Found: C, 77.02; H, 10.16; N, 5.13%. ^{1}H-NMR (benzene-d_6, 200 MHz): δ 3.92 (sept., $^3J(^1H, {}^1H) = 6.8$ Hz, 2H, NCH(CH$_3$)$_2$), 3.15 (sept., $^3J(^1H, {}^1H) = 7.1$ Hz, 2H, CpCH(CH$_3$)$_2$), 2.25 (s, 12H, Cp(CH_3)$_2$), 2.14 (s, 12H, Cp(CH_3)$_2$), 1.59 (s, 6H, NC(CH_3)), 1.41 (d, $^3J(^1H, {}^1H) = 7.1$ Hz, 12H, CpCH(CH_3)$_2$), 1.27 (d, $^3J(^1H, {}^1H) = 6.8$ Hz, 12H, NCH(CH_3)$_2$). ^{13}C$\{^1$H$\}$ (benzene-d_6, 50.32 MHz): δ 195.93 (NCN), 124.54 (NCCH$_3$), 122.38 (C_5CHCH$_3$), 112.79 (C_5CH$_3$), 112.56 (C_5CH$_3$), 52.86 (NCH), 27.46 (C_5CHCH$_3$), 24.13 (NCHCH$_3$), 23.14 (CCHCH$_3$) 13.08 (C$_5$$CH_3$), 12.03 (C$_5$$CH_3$), 10.01 (C$CH_3$). MS (EI, ^{40}Ca, 105°C): m/z 366 (38%) [M $-$ C$_{11}$H$_{20}$N$_2$]$^+$, 203 (100%) [C$_{12}$H$_{19}$Ca]$^+$, 180 (31%) [C$_{11}$H$_{20}$N$_2$]$^+$, 163 (43%) [C$_{12}$H$_{19}$]$^+$.

4.2.11. (C$_5$Me$_5$)$_2$(iPr-carbene)Sr (12)

Analogously to **10**, 0.84 g (1.7 mmol) of (C$_5$Me$_5$)$_2$(THF)$_2$Sr was reacted with 0.31 g (1.7 mmol) of *i*Pr-carbene in 30 ml of toluene. After concentrating the solvent in vacuo (10^{-2} hPa) to 10 ml, **12** crystallized at $-20\,^{\circ}$C as colorless crystals. Yield: 0.50 g (55%). M.p.: 148°C. Anal. Calc. for $C_{31}H_{50}N_2Sr$: C, 69.19; H, 9.36; N, 5.20. Found: C, 68.16; H, 9.69; N, 5.52%. ^{1}H-NMR (benzene-d_6, 200 MHz): δ 3.7–3.5 (m, 2H, NCH(CH$_3$)$_2$), 2.16 (s, 30H, Cp(CH_3)$_5$), 1.52 (s, 6H, NCCH_3), 1.2–1.0 (m, 12H, NCHCH_3). ^{13}C$\{^1$H$\}$ (benzene-d_6, 50.32 MHz): δ n.f. (NCN), 125.23 (NCCH$_3$), 111.41 (C_5CH$_3$), 48.57 (NCH), 20.96 (NCHCH$_3$), 11.29 (C$_5$$CH_3$), 8.17 (C$CH_3$). MS (EI, 205°C, ^{88}Sr): m/z 358 (8%) [M $-$ C$_{11}$H$_{20}$N$_2$]$^+$, 223 (37%) [C$_{10}$H$_{15}$Sr], 180 (17%) [C$_{11}$H$_{20}$N$_2$]$^+$, 136 (43%) [C$_{10}$H$_{16}$]$^+$. MS (CI, ^{88}Sr, CA He 5.5): m/z 538 [M]$^+$, 403 [M $-$ C$_{10}$H$_{15}$]$^+$, 358 [M $-$ C$_{11}$H$_{20}$N$_2$]$^+$, 268 [C$_{11}$H$_{20}$N$_2$Sr]$^+$.

4.2.12. (C$_5$Me$_4$tBu)$_2$(THF)$_2$Ba (13)

To 0.65 g (4.7 mmol) of Ba pieces in 30 ml of THF was added 1.69 g (9.5 mmol) of C$_5$Me$_4$tBuH. Ammonia was condensed at $-78\,^{\circ}$C into this mixture for 20 min under dissolving the Ba and forming a golden solid. After stirring for 3 h at $-78\,^{\circ}$C, the mixture was warmed up to 25°C and stirred for another 12 h. The white slurry was separated from the gray solid and the solvent removed in vacuo (10^{-2} hPa). Additionally the white solid was extracted continuously with 50 ml of toluene for 48 h and afterwards the solvent was reduced to 15 ml. Crystallization at $-20\,^{\circ}$C yields **13** as a colorless microcrystalline solid. Yield: 2.51 g (84%). M.p.: 180°C. Anal. Calc. for $C_{34}H_{58}BaO_2$: C, 64.19; H, 9.19. Found: C, 62.53; H, 9.15%. ^{1}H-NMR (pyridine-d_5, 400 MHz): δ 3.65 (m, 8H, THF), 2.16 (s, 12H, Cp(CH_3)$_2$), 2.05 (s, 12H, Cp(CH_3)$_2$), 1.61 (m, 8H, THF), 1.46 (s, 18H, C(CH_3)$_3$). ^{13}C$\{^1$H$\}$ (pyridine-d_5, 100.64 MHz): δ 124.88 (C_5CCH$_3$), 113.27 (C_5CH$_3$), 111.63 (C_5CH$_3$), 67.53 (THF), 34.61 (CCH$_3$), 33.19 (CCH$_3$), 25.45 (THF), 14.80 (C$_5$$CH_3$), 11.32 (C$_5$$CH_3$). MS (EI, ^{138}Ba, 176°C): m/z 492 (4%) [M $-$ 2THF]$^+$, 315 (38%) [C$_{13}$H$_{21}$Ba]$^+$, 178 (30%) [C$_{13}$H$_{22}$]$^+$.

4.2.13. (C$_5$Me$_4$tBu)$_2$(pyridine)$_2$Ba (14)

0.71 g (1.1 mmol) of **13** was dissolved in 15 ml of pyridine and stirred for 2 h. Crystallization at $-20\,^{\circ}$C yields **14** as yellow crystals. Yield: 0.55 g (76%). M.p.: 270°C. Anal. Calc. for $C_{36}H_{52}BaN_2$: C, 66.51; H, 8.06; N, 4.31. Found: C, 65.65; H, 10.04; N, 5.72%. ^{1}H-NMR (pyridine-d_5, 400 MHz): δ 8.72 (m, 4H, pyridine), 7.56 (m, 2H, pyridine), 7.19 (m, 4H, pyridine), 2.15 (s, 12H, Cp(CH_3)$_2$), 2.07 (s, 12H, Cp(CH_3)$_2$), 1.45 (s, 18H, C(CH_3)$_3$). ^{13}C$\{^1$H$\}$ (pyridine-d_5, 100.64 MHz): δ 149.97 (pyridine), 135.70 (pyridine), 124.87 (C_5CCH$_3$), 123.70 (pyridine), 113.27 (C_5CH$_3$), 111.60 (C_5CH$_3$), 34.54 (CCH$_3$), 33.22 (CCH$_3$), 14.68 (C$_5$$CH_3$), 11.33 (C$_5$$CH_3$).

Table 2
Summary of X-ray data for **1**, **2**, **4**, **6**, **9**, **10**, **11**, **12**, **14**, and **15**

Compound	**1**	**2**	**4**
Empirical formula	$C_{18}H_{26}Mg$	$C_{26}H_{42}Mg$	$C_{29}H_{46}MgN_2$
Formula weight	226.70	378.91	446.99
Crystal system	Monoclinic	Monoclinic	Monoclinic
Space group	$P2_1/n$ (no. 14)	$C2/c$ (no. 15)	$P2_1/n$ (no. 14)
Unit cell parameters			
a (Å)	8.4478(1)	14.9805(3)	10.8367(1)
b (Å)	8.1504(1)	10.0840(2)	15.7188(3)
c (Å)	12.2838(2)	31.6779(5)	16.1474(2)
β (°)	105.989(1)	95.242(1)	91.944(1)
Volume (Å³)	813.056(19)	4765.36(15)	2748.96(7)
Z	2	8	4
D_{calc} (g cm⁻³)	1.089	1.056	1.080
μ(Mo–K$_\alpha$) (mm⁻¹)	0.095	0.082	0.082
$F(000)$	292	1680	984
Crystal size (mm³)	$0.78 \times 0.68 \times 0.52$	$0.60 \times 0.53 \times 0.13$	$0.76 \times 0.50 \times 0.44$
Crystal habit	Block	Plate	Block
θ_{min}, θ_{max} (°)	3.04, 30.55	1.29, 27.50	1.81, 27.50
Index ranges	$-12 \leq h \leq 11$	$-19 \leq h \leq 19$	$-14 \leq h \leq 13$
	$-11 \leq k \leq 7$	$-10 \leq k \leq 13$	$-20 \leq k \leq 14$
	$-16 \leq l \leq 17$	$-40 \leq l \leq 41$	$-17 \leq l \leq 20$
Reflections collected	7267	17485	20067
Independent reflections	2472 [$R_{int} = 0.0417$]	5444 [$R_{int} = 0.0713$]	6255 [$R_{int} = 0.0334$]
Max., min. transmission			0.9512, 0.7775
Data, restraints, parameters	2472, 0, 92	5444, 0, 258	6255, 0, 303
Goodness-of-fit	1.083	1.158	1.030
R_1, wR_2, $I > 2\sigma(I)$ [a]	0.0406, 0.1160	0.0755, 0.1710	0.0433, 0.1150
All data	0.0473, 0.1230	0.0972, 0.1863	0.0595, 0.1271
Absolute structure parameter			
Largest difference peak, hole (e Å⁻³)	0.267, −0.300	0.423, −0.325	0.307, −0.222

Compound	**6**	**9**	**10**
Empirical formula	$C_{18}H_{32}CaN_2 \cdot C_4H_8O$	$C_{28}H_{46}CaO$	$C_{49}H_{46}N_2Ca$
Formula weight	388.64	438.73	462.76
Crystal system	Orthorhombic	Trigonal	Orthorhombic
Space group	$P2_12_12_1$ (no. 19)	$P3_121$ (no. 152)	$P2_12_12_1$ (no. 19)
Unit cell parameters			
a (Å)	9.8929(1)	15.3145(1)	10.7658(1)
b (Å)	12.2999(2)	15.3145(1)	13.1087(1)
c (Å)	19.2015(3)	9.8503(1)	20.0137(1)
β (°)	90	90	90
Volume (Å³)	2336.47(6)	2000.72(3)	2824.45(4)
Z	4	3	4
D_{calc} (g cm⁻³)	1.105	1.092	1.088
μ(Mo–K$_\alpha$) (mm⁻¹)	0.281	0.251	0.240
$F(000)$	856	726	1016
Crystal size (mm³)	$0.90 \times 0.80 \times 0.75$	$0.90 \times 0.62 \times 0.56$	$0.56 \times 0.46 \times 0.10$
Crystal habit	Block	Block	Plate
θ_{min}, θ_{max} (°)	1.97, 30.48	1.54, 27.50	1.86, 25.50
Index ranges	$-13 \leq h \leq 14$	$-17 \leq h \leq 19$	$-10 \leq h \leq 13$
	$-14 \leq k \leq 17$	$-19 \leq k \leq 19$	$-14 \leq k \leq 15$
	$-22 \leq l \leq 27$	$-12 \leq l \leq 12$	$-24 \leq l \leq 21$
Reflections collected	22094	15214	18719
Independent reflections	7089 [$R_{int} = 0.0369$]	3069 [$R_{int} = 0.0789$]	5220 [$R_{int} = 0.1077$]
Max., min. transmission	0.8481, 0.7038	0.9799, 0.3341	0.9779, 0.2729
Data, restraints, parameters	7089, 0, 245	3069, 0, 143	5220, 0, 303
Goodness-of-fit	1.028	1.039	1.002
R_1, wR_2, $I > 2\sigma(I)$ [a]	0.0386, 0.0972	0.0410, 0.1061	0.0577, 0.1204
All data	0.0444, 0.1012	0.0506, 0.1127	0.0840, 0.1314
Absolute structure parameter	0.01(2)	0.02(6)	0.03(5)
Largest difference peak, hole (e Å⁻³)	0.610, −0.453	0.266, −0.380	0.482, −0.505

Table 2 (*Continued*)

Compound	**11**	**12**	**14**
Empirical formula	$C_{35}H_{58}CaN_2 \cdot \frac{1}{2}C_7H_8$	$C_{31}H_{50}N_2Sr \cdot \frac{1}{2}C_7H_8$	$C_{36}H_{52}BaN_2 \cdot \frac{1}{2}C_5H_5N$
Formula weight	592.98	584.42	689.69
Crystal system	Monoclinic	Monoclinic	Monoclinic
Space group	$P2_1/c$ (no. 14)	$I2/a$ (no. 15)	$P2_1/c$ (no. 14)
Unit cell parameters			
a (Å)	17.2594(2)	18.4520(10)	9.6394(1)
b (Å)	25.6229(3)	19.2090(10)	19.7524(2)
c (Å)	18.2022(2)	18.7610(10)	19.5242(2)
β (°)	112.395(1)	92.180(10)	95.093(1)
Volume (Å³)	7442.55(15)	6644.9(6)	3702.67(7)
Z	8	8	4
D_{calc} (g cm⁻³)	1.058	1.168	1.237
μ(Mo–K$_\alpha$) (mm⁻¹)	0.195	1.646	1.099
$F(000)$	2616	2504	1436
Crystal size (mm³)	$0.90 \times 0.70 \times 0.50$	$0.36 \times 0.24 \times 0.24$	$0.77 \times 0.64 \times 0.30$
Crystal habit	Prism	Block	Block
θ_{min}, θ_{max} (°)	1.28, 27.50	1.52, 23.00	2.12, 27.50
Index ranges	$-21 \leq h \leq 22$	$-20 \leq h \leq 16$	$-11 \leq h \leq 12$
	$-33 \leq k \leq 33$	$-21 \leq k \leq 16$	$-24 \leq k \leq 25$
	$-23 \leq l \leq 12$	$-20 \leq l \leq 17$	$-25 \leq l \leq 25$
Reflections collected	54692	8765	27455
Independent reflections	17037 [$R_{int} = 0.0727$]	4583 [$R_{int} = 0.1156$]	4583 [$R_{int} = 0.0427$]
Max., min. transmission	0.9318, 0.5604		0.7845, 0.5320
Data, restraints, parameters	17037, 0, 785	4583, 0, 357	8478, 14, 390
Goodness-of-fit	1.024	1.002	1.061
R_1, wR_2, $I > 2\sigma(I)$ [a]	0.0682, 0.1676	0.0509, 0.0947	0.0389, 0.0875
All data	0.1264, 0.2046	0.1190, 0.1131	0.0561, 0.0966
Absolute structure parameter			
Largest difference peak, hole (e Å⁻³)	0.726, −0.469	0.619, −0.790	0.910, −0.627

Compound	**15**
Empirical formula	$C_{37}H_{62}BaN_2 \cdot C_7H_8$
Formula weight	764.36
Crystal system	Orthorhombic
Space group	$Pbcn$ (no. 60)
Unit cell parameters	
a (Å)	25.1722(3)
b (Å)	21.1318(2)
c (Å)	15.7648(2)
β (°)	90
Volume (Å³)	8385.83(17)
Z	8
D_{calc} (g cm⁻³)	1.211
μ(Mo–K$_\alpha$) (mm⁻¹)	0.977
$F(000)$	3232
Crystal size (mm³)	$0.92 \times 0.46 \times 0.44$
Crystal habit	Block
θ_{min}, θ_{max} (°)	1.62, 27.50
Index ranges	$-26 \leq h \leq 32$
	$-27 \leq k \leq 27$
	$-20 \leq l \leq 20$
Reflections collected	59708
Independent reflections	9622 [$R_{int} = 0.0567$]
Max., min. transmission	0.7297, 0.5435
Data, restraints, parameters	9622, 0, 445
Goodness-of-fit	1.144
R_1, wR_2, $I > 2\sigma(I)$ [a]	0.0384, 0.0709
All data	0.0635, 0.0830
Absolute structure parameter	
Largest difference peak, hole (e Å⁻³)	1.003, −0.655

[a] $R_1 = \Sigma ||F_o| - |F_c|| / \Sigma |F_o|$; $wR_2 = [\Sigma w(F_o^2 - F_c^2)^2 / \Sigma w(F_o^2)^2]^{1/2}$.

MS (EI, ^{138}Ba, 155°C): m/z 492 (16%) [M − 2pyridine]$^+$, 315 (100%) [$C_{13}H_{21}Ba$]$^+$, 178 (5%) [$C_{13}H_{22}$]$^+$.

4.2.14. $(C_5Me_4tBu)_2(iPr\text{-}carbene)Ba$ (15)

To 1.10 g (1.7 mmol) of **13**, dissolved in 50 ml of toluene was added 0.31 g (1.7 mmol) of iPr-carbene in portions. The mixture was stirred for 12 h under reflux and was concentrated in vacuo (10^{-2} hPa) to 10 ml. Crystallization at − 20°C gave **15** as colorless crystals. Yield: 0.97 g (85%). M.p.: 156°C. Anal. Calc. for $C_{37}H_{62}BaN_2$: C, 66.11; H, 9.30; N, 4.17. Found: C, 66.99; H, 9.36; N, 5.28%. ^{1}H-NMR (benzene-d_6, 200 MHz): δ 3.78 (sept., $^3J(^1H, {}^1H) = 6.6$ Hz, 2H, NC*H*CH$_3$), 2.37 (s, 12H, CpC*H*$_3$), 2.06 (s, 12H, CpC*H*$_3$), 1.58 (s, 18H, CC*H*$_3$), 1.57 (s, 12H, NCC*H*$_3$), 1.18 (d, $^3J(^1H, {}^1H) = 6.6$ Hz, 12H, NCHC*H*$_3$). ^{13}C{^{1}H} (benzene-d_6, 100.64 MHz): δ 200.24 (N*C*N), 125.29 (C_5CCH$_3$), 123.72 (N*C*CH$_3$), 114.69 (C_5CH$_3$), 112.62 (C_5CH$_3$), 49.12 (N*C*H), 35.25 (*C*CH$_3$), 33.68 (C*C*H$_3$), 23.45 (NCH*C*H$_3$), 15.37 (C_5*C*H$_3$), 11.73 (C_5*C*H$_3$), 8.90 (C*C*H$_3$). MS (EI, ^{138}Ba, 130°C): m/z 492 (11%) [M − $C_{11}H_{20}N_2$]$^+$, 315 (31%) [$C_{13}H_{21}Ba$]$^+$, 180 (58%) [$C_{11}H_{20}N_2$]$^+$, 178 (90%) [$C_{13}H_{22}$]$^+$.

4.3. X-ray structure determination

The crystal data and details of data collection are given in Table 2. Data were collected on a Siemens SMART CCD diffractometer (graphite monochromated Mo−K$_\alpha$ radiation, $\lambda = 0.71073$ Å) with area-detector by use of ω scans at 173 K for **1**, **2**, **4**, **6**, **9**, **10**, **11**, **14**, and **15**. Data of **12** were collected on an Enraf Nonius CAD-4 diffractometer (graphite monochromated Mo−K$_\alpha$ radiation, $\lambda = 0.71073$ Å) by the use of ω−2θ scans at 163 K. The structures were solved by direct methods using SHELXS-97 [33] and refined on F^2 using all reflections with SHELXL-97 [34]. The carbon and the nitrogen atoms of the disordered pyridine solvent in **14** were refined isotropically, all other non-hydrogen atoms anisotropically. The hydrogen atoms were placed in calculated positions and assigned to an isotropic displacement parameter of 0.08 Å^2. The idealized methyl-groups were allowed to rotate about their X−C bond. Absolute structure parameters were determined according to Flack [35] with SHELXL-97. SADABS [36] was used to perform area-detector scaling and absorption corrections for **4**, **6**, **10**, **11**, **14** and **15**. The maximum and minimum transmission factors are summarized in Table 2. The geometrical aspects of the structures were analyzed by using the PLATON program [37].

The asymmetric unit of **14** contains a pyridine molecule which is disordered about a center of inversion. All C−C and C−N distances were refined with idealized bond distances of 1.375 Å and 1.330 Å respectively (DFIX). Furthermore the atoms of the solvent molecule were restrained to lie on a common plane. The toluene solvent molecule in **12** is disordered about a center of inversion. For clarity, all hydrogen atoms in the ORTEP plots [12] except those on the nitrogen atoms in Fig. 4 are removed.

5. Supplementary material

Crystallographic data for structural analysis have been deposited with the Cambridge Crystallographic Data Center, CCDC nos. 147800 (**1**), 147801 (**2**), 147802 (**4**), 147803 (**6**), 147804 (**9**), 147805 (**10**), 147806 (**11**), 147807 (**12**), 147808 (**14**), and 147809 (**15**). Copies of this information may be obtained free of charge from The Director, CCDC, 12 Union Road, Cambridge, CB2 1EZ, UK (Fax: + 44-1223-336033; e-mail: deposit@ccdc.cam.ac.uk or www: http://www.ccdc. cam.ac.uk).

References

[1] H.W. Wanzlick, Angew. Chem. 74 (1962) 129; Angew. Chem. Int. Ed. Engl. 1 (1962) 75.

[2] A.J. Arduengo, III, R.L. Harlow, M. Kline, J. Am. Chem. Soc. 113 (1991) 361.

[3] D. Bourissou, O. Guerret, F.P. Gabbai, G. Bertrand, Chem. Rev. 100 (2000) 39 and refs. cited therein.

[4] N. Kuhn, T. Kratz, G. Henkel, J. Chem. Soc. Chem.Commun. (1993) 1778.

[5] N. Kuhn, T. Kratz, D. Bläser, R. Boese, Chem. Ber. 128 (1995) 245.

[6] N. Kuhn, G. Henkel, T. Kratz, J. Kreutzberg, R. Boese, A.H. Maulitz, Chem. Ber. 126 (1993) 2041. C.J. Carmalt, A.H. Cowley, Adv. Inorg. Chem. 50 (2000) 1.

[7] (a) H. Schumann, M. Glanz, J. Winterfeld, H. Hemling, N. Kuhn, T. Kratz, Angew. Chem. 106 (1994) 1829; Angew. Chem. Int. Ed. Engl. 33 (1994) 1733. (b) H. Schumann, M. Glanz, J. Winterfeld, H. Hemling, N. Kuhn, T. Kratz, Chem. Ber. 127 (1994) 2369. (c) A.J. Arduengo III, M. Tamm, S.J. McLain, C.J. Calabrese, F. Davidson, W.J. Marshall, J. Am. Chem. Soc. 116 (1994) 7927. (d) W.A. Herrmann, F.C. Munck, G.R.J. Artus, O. Runte, R. Anwander, Organometallics 16 (1997) 682.

[8] A.J. Arduengo, III, H.V.R. Dias, F. Davidson, R.L. Harlow, J. Organomet. Chem. 462 (1993) 13.

[9] W.A. Herrmann, C. Köcher, Angew. Chem. 109 (1997) 2256; Angew. Chem. Int. Ed. Engl. 36 (1997) 2162.

[10] A.J. Arduengo, III, F. Davidson, R. Krafczyk, W.J. Marshall, M. Tamm, Organometallics 17 (1998) 3375.

[11] H. Schumann, M. Glanz, J. Gottfriedsen, S. Dechert, D. Wolff, Pure Appl. Chem. in press.

[12] L. Zolnai, H. Pritzkow, ZORTEP, ORTEP-Program for PC, Universität Heidelberg, 1994.

[13] W. Bünder, E. Weiss, J. Organomet. Chem. 92 (1975) 1.

[14] (a) S. Evans, M.L.H. Green, B. Jewitt, A.F. Orchard, C.F. Pyall, J. Chem. Soc. Faraday Trans. 68 (1972) 1847. (b) J.L. Robbins, N. Edelstein, B. Spencer, J.C. Smart, J. Am. Chem. Soc. 104 (1982) 1882. (c) R.A. Andersen, R. Blom, J.M. Boncella, J.C. Burns, H.V. Volden, Acta Chem. Scand. A 41 (1987) 24.

[15] M.G. Gardiner, C.L. Raston, C.H.L. Kennard, Organometallics 10 (1991) 3680.

[16] C.P. Morley, P. Jutzi, C. Krüger, J.M. Wallis, Organometallics 6 (1987) 1084.

[17] (a) M. Kirilov, G. Petrov, C. Angelov, J. Organomet. Chem. 113 (1976) 225. (b) S.R. Drake, D.J. Otway, Polyhedron 11 (1992) 745. (c) S.R. Drake, D.J. Otway, J. Chem. Soc. Chem. Commun. (1991) 517.

[18] (a) L.M. Engelhardt, P.C. Junk, C.L. Raston, A.H. White, J. Chem. Soc. Chem. Commun. (1988) 1500. (b) P. Jutzi, W. Leffers, G. Müller, B. Huber, Chem. Ber. 122 (1989) 879.

[19] A. Hammel, W. Schwarz, J. Weidlein, J. Organomet. Chem. 378 (1989) 347.

[20] G.A. Molander, H. Schumann, E.C.E. Rosenthal, J. Demtschuk, Organometallics 15 (1996) 3817.

[21] F.A. Mautner, H. Krischner, Z. Kristallogr. 176 (1986) 85.

[22] G. Mösgen, F. Hampel, M. Kaupp, P. von Rague Schleyer, J. Am. Chem. Soc. 114 (1992) 10880.

[23] D. Burkey, T.P. Hanusa, Acta Crystallogr. Sect. C 52 (1996) 2452.

[24] D.J. Burkey, R.A. Williams, T.P. Hanusa, Organometallics 12 (1993) 1331.

[25] R.A. Williams, T.P. Hanusa, J.C. Huffman, J. Organomet. Chem. 429 (1992) 143.

[26] R.D. Shannon, Acta Crystallogr. Sect. A 32 (1976) 751.

[27] C.A. Schalley, D. Schröder, H. Schwarz, Int. J. Mass Spectrom. Ion Processes 153 (1996) 173.

[28] (a) K.E. de Plooy, J. du Toit, D.C. Demetrius, N.J. Coville, J. Organomet. Chem. 508 (1996) 231. (b) H. Schumann, K. Zietzke, F. Erbstein, R. Weimann, J. Organomet. Chem. 520 (1996) 265.

[29] J. Okuda, Chem. Ber. 122 (1989) 1075.

[30] H. Schumann, M.R. Keitsch, J. Winterfeld, S. Mühle, G.A. Molander, J. Organomet. Chem. 559 (1998) 181.

[31] M.J. McCormick, R.A. Williams, L.J. Levine, T.P. Hanusa, Polyhedron 7 (1988) 725.

[32] N. Kuhn, T. Kratz, Synthesis (1993) 561.

[33] G.M. Sheldrick, SHELXS-97, Program for the Solution of Crystal Structures, University of Göttingen, Germany, 1990.

[34] G.M. Sheldrick, SHELXL-97, Program for the Refinement of Crystal Structures, University of Göttingen, Germany, 1997.

[35] H.D. Flack, Acta Crystallogr. Sect. A 39 (1983) 876.

[36] G.M. Sheldrick, SADABS, Program for Empirical Absorption Correction of Area Detector Data, University of Göttingen, Germany, 1996.

[37] A.L. Spek, Acta Crystallogr. Sect. A 46 (1990) 34.